Supplemental Online Materials for Lea et al.

Materials and methods

Preparation of samples and determination of Mg/Ca: 25-30 individuals of *G. ruber*-white variety were picked from the 250-350 μm fraction of the coarse fraction for each analysis. In about 25% of the intervals, white and pink varieties were combined for analysis because the white variety alone were of insufficient abundance. Comparison of Mg/Ca in pink and white varieties revealed no obvious differences. In a few intervals, most notably between 510-630 cm within the Bølling/Allerød (B/A) time interval, it was necessary to also relax the size definition because of very low *G. ruber* abundances. The same practice was followed previously for stable isotope analysis in PL07-39PC (*S1*). Separate replicate preparations and analyses of Mg/Ca were made on the two-thirds of the intervals which had sufficient abundances. The average weight of *G. ruber* shells was 12.5 μg. There are subtle variations in shell weight throughout the core, from a minimum of ~10 μg at 300 cm to a maximum of ~13 μg between 760-965 cm. There is no correlation between Mg/Ca and shell weight, and there are no sharp changes in shell weight matching the transitions in Mg/Ca.

Shell samples were gently crushed and cleaned using the UCSB standard foraminifera cleaning procedure without the DTPA step (*S2, S3*). Dissolved samples were analyzed by the isotope dilution/internal standard method described in (*S2*) using a Thermo Finnigan Element2 sector ICP-MS. Analytical reproducibility, assessed by analyzing consistency standards matched in concentration and Mg/Ca ratio to dissolved foraminifera solutions and analyzed over the course of the entire study (~18 months), is estimated at ±0.7% (1 σ). The pooled standard deviation of replicate analyses from PL07-39PC was ±4.1% (1 SD, df =155). Less than 2% of the individual analyses were rejected as outliers. The overall precision of replicates for PL07-39PC was slightly worse than other tropical cores we have analyzed (typically ~3% (*S2*)), mostly because of significantly poorer reproducibility between 510-630 cm, the B/A time interval. Oxygen isotope analyses on PL07-39PC also exhibit poorer consistency in this interval (*S1*). This might result from having used a broader size fraction in this interval (see above). Elemental ratios of Mn/Ca, Fe/Ca and Al/Ca were analyzed at the same time as Mg/Ca to assess cleaning efficacy. Both Mn/Ca and Fe/Ca are substantially elevated in the massive, bioturbated section below 630 cm, but Al/Ca was uniformly low throughout the entire core, typically <10 μmol/mol, indicating that detrital contamination of Mg is not a cleaning issue at this site. There is no correlation between Mg/Ca and either Mn/Ca, Fe/Ca or Al/Ca. Elevated Mn/Ca and Fe/Ca levels below 630 cm are most likely due to the influence of sub-oxic diagenesis on shell coatings (*S4*) in this time interval.

Calendar age model for PL07-39PC: the chronology was developed from available radiocarbon dates (*S1*) and grayscale record (*S5*). All depths are given as uncorrected for the turbidite between 170-190 cm (*S1*). Eight radiocarbon dates, converted to calibrated radiocarbon ages assuming a reservoir age of 420 years (*S5, S6*) and Calib v. 4.4 (*S7*, *S8*), were used to develop the age model between the core-top and 215 cm (to 7805 y BP). From 220-335 cm, we used five tie-points between the grayscale record of 39PC and

56PC, which has been placed on a varve chronology (*S9, S10*). These tie-points are based on the most obvious large-scale features in the two records, which are very similar (Fig. S1). Two additional radiocarbon dates were used at 287 and 307 cm because the grayscale match is not obvious in this interval. Ten tie-points between the grayscale records were used between 330 and 630 cm, where the transitions are very clear (*S5*). The worst discrepancy between ages derived from the grayscale matches and available radiocarbon ages in these same intervals was 750 y, but the average difference was 310 y. Below 630 cm the sediment is massively bioturbated, and four additional radiocarbon ages were used to develop an age model. The complete age model is given in Table S1. A complete data listing on both depth and age is given in Table S2.

Supplemental Text on Comparison of Proxy Temperature Records
The 2.6±0.5°C glacial – interglacial change in SST implied by Mg/Ca can account for ~ 0.6‰ change in $\delta^{18}O$ (*S11*), whereas the observed change is ~2‰. Assuming a 1‰ change due to global ice volume (*S12*), the residual change (~0.4‰) implies a local or regional increase in salinity, in agreement with independent faunal and isotopic evidence for saltier conditions in the Caribbean during the LGM (*S13, S14*). Previous estimates of SST change based on comparison of isotope records from *G. ruber* and deeper-dwelling planktonic species suggested a 3-4°C cooling (*S1*), in good agreement with the Mg/Ca-based estimate. An alternative SST record based on alkenone unsaturation measurements does not indicate significant cooling in either the YD or LGM chronozones (*S15*). There is no obvious reason for this discrepancy, but if alkenone unsaturation temperatures are recording upwelling conditions, as might be expected for bloom organisms such as coccolithophorids, then the additional complication of sea level modulation of sill depth would affect those temperatures. In fact, the much smaller glacial-interglacial change in *Globigerina bulloides* and *Neogloboquadrina dutertrei* $\delta^{18}O$ was previously explained as a consequence of shallower (and hence, on a relative basis, warmer) source waters feeding upwelling during sea level low stands (*S1*).

Point-to-point comparison of Mg/Ca-SST and $\delta^{18}O$ over the three major deglacial transitions indicates a generally good correspondence, although the transitions are much less clearly defined in the $\delta^{18}O$ record. Over the Bølling transition, the change in SST is +3°C and -0.8‰ in $\delta^{18}O$; over the YD onset, the change in SST is -3.5°C and +0.5‰ in $\delta^{18}O$; and, over the YD termination, the change in SST is +3.5°C and -0.65‰ in $\delta^{18}O$. In all three cases, assuming -0.2‰ $\delta^{18}O$ change per °C (*S11*), the $\delta^{18}O$ change is within 0.2‰ of the change expected from temperature alone.

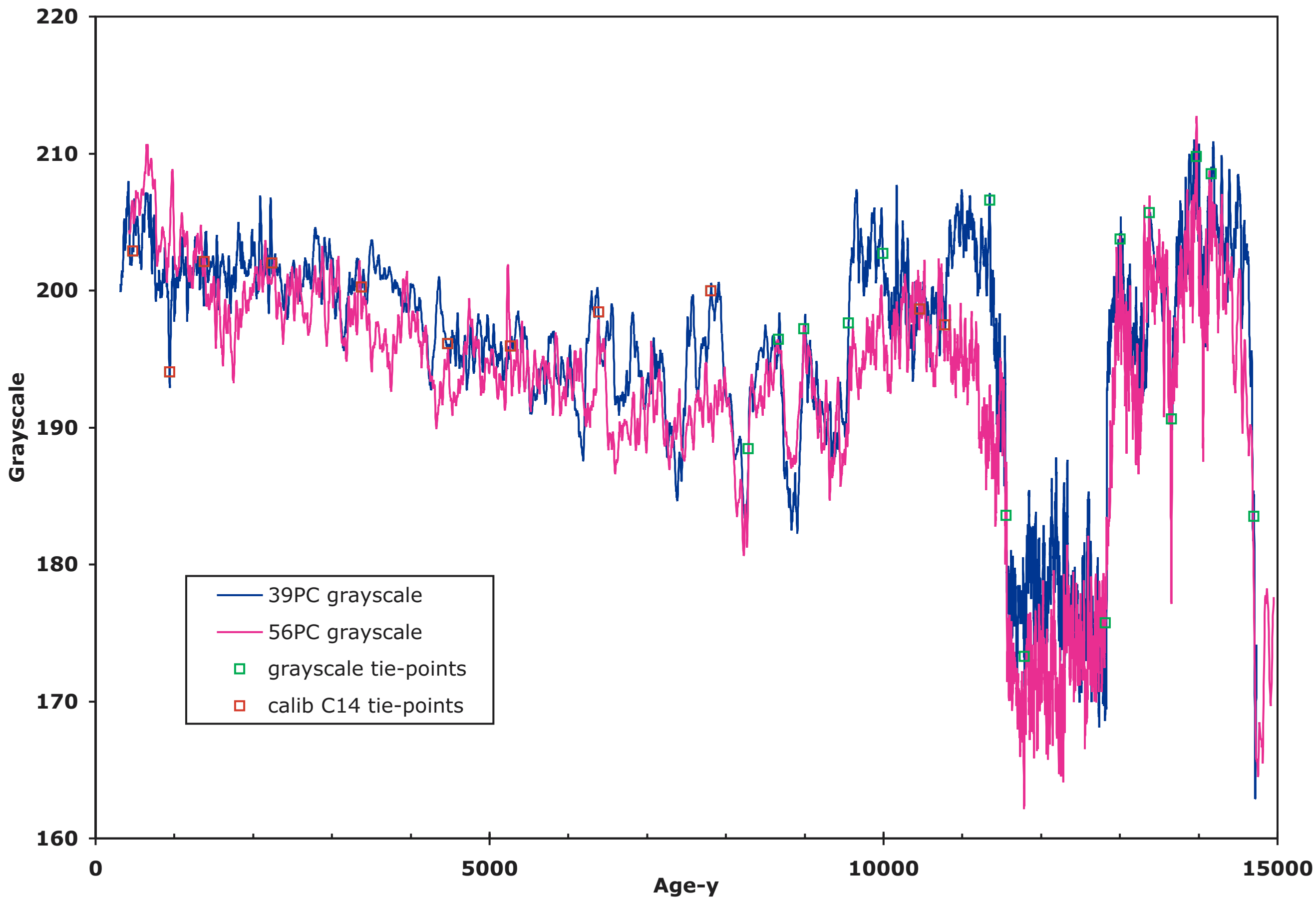

Fig. S1: Grayscale records for PL07-39PC and PL07-56PC (*S5*) on a calendar age scale (Table S1). Age control points based on calibrated radiocarbon ages in PL07-39PC are indicated by red squares. Age control points based on matching the grayscale record of PL07-39PC to PL07-56PC are indicated by green squares. See (*S5)* for a comparison of the records on depth scales.

Table S1: complete age model for PL07-39PC

Depth 39PC UNCORR	Cal age 39PC tie points	sedimentation rate (cm/ky)*	Source
7	477		calib C14†
26	945	40.6	calib C14
45	1383	43.4	calib C14
74.5	2238	34.5	calib C14
104	3378	25.9	calib C14
120	4468	14.7	calib C14
144	5268	30.0	calib C14
165	6385	18.8	calib C14
214.5	7809	20.7	calib C14
222.78	8286.4	17.3	grayscale match
228.6	8667	15.3	grayscale match
237.19	8992.2	26.4	grayscale match
251.82	9558	25.9	grayscale match
266.2	9992	33.1	grayscale match
294	10464	58.9	calib C14
307	10780	41.1	calib C14
331.37	11352	42.6	grayscale match
355.73	11556	119.4	grayscale match
373.09	11786	75.5	grayscale match
502.09	12817	125.1	grayscale match
520.09	13007	94.7	grayscale match
552.33	13373	88.1	grayscale match
556.34	13658	14.1	grayscale match
577.39	13970	67.5	grayscale match
599.68	14160	117.3	grayscale match
627.66	14704	51.4	grayscale match
723.5	16180	64.9	calib C14
771.5	17117	51.2	calib C14
903.5	20361	40.7	calib C14
982.5	24382	19.6	calib C14

†Calibrated ages calculated using Calib v. 4.4 with $\Delta R=0$; age is the median probability age.

*Sedimentation rate is calculated between the preceding depth and the next depth.

Table S2: complete data listing for core PL07-39PC

Depth (cm)	**Age (y)**	**Mg/Ca (m)**	**SST (°C)**
0	305	4.267	26.9
6.5	465	4.108	26.5
10	551	4.109	26.5
16.5	711	4.301	27.0
20	797	4.220	26.7
26	945	4.244	26.8
30	1037	4.290	26.9
36.5	1187	4.145	26.5
40	1268	4.131	26.5
45	1383	4.204	26.7
50	1528	4.259	26.9
55	1673	4.273	26.9
60	1818	4.487	27.4
65	1963	4.383	27.2
70	2108	3.966	26.1
75	2257	4.237	26.8
80	2451	4.085	26.4
85	2644	4.218	26.7
90	2837	4.170	26.6
95	3030	4.279	26.9
100	3223	4.334	27.0
105	3446	4.081	26.4
110	3787	3.966	26.1
115	4127	4.031	26.2
120	4468	4.066	26.3
125	4635	4.240	26.8
130	4801	4.071	26.3
135	4968	4.313	27.0
140	5135	4.108	26.4
145	5321	3.959	26.0
150	5587	4.109	26.5
154	5800	4.043	26.3
160	6119	3.927	25.9
165	6385	4.261	26.9
195	6868	4.362	27.1
200	7109	4.431	27.3
205	7350	4.437	27.3
210	7592	4.076	26.4
215	7838	4.615	27.7
220	8126	4.372	27.1
225	8432	4.361	27.1
230	8720	4.236	26.8

235	8909	4.197	26.7
240	9101	4.309	27.0
245	9294	4.029	26.2
256	9684	4.414	27.2
260	9805	4.591	27.7
265	9956	4.579	27.7
270	10057	4.222	26.8
275	10141	4.184	26.7
280	10226	4.111	26.5
285	10311	4.219	26.7
290	10396	4.011	26.2
297	10537	4.363	27.1
300	10610	4.103	26.4
305	10731	4.450	27.3
312	10897	4.201	26.7
316	10991	4.327	27.0
320	11085	3.867	25.8
325	11202	3.877	25.8
330	11320	4.444	27.3
336	11391	4.638	27.8
340	11424	3.903	25.9
345	11466	4.022	26.2
350	11508	3.666	25.2
355	11550	3.875	25.8
360	11613	3.393	24.3
365	11679	3.477	24.6
370	11745	3.305	24.0
375	11801	3.615	25.0
380	11841	3.219	23.7
385	11881	3.181	23.6
390	11921	3.490	24.6
395	11961	3.306	24.0
400	12001	3.376	24.3
406	12049	3.608	25.0
410	12081	3.121	23.4
415	12121	3.537	24.8
420	12161	3.317	24.1
425	12201	3.339	24.1
430	12241	3.502	24.7
435	12281	3.409	24.4
445	12361	3.002	23.0
450	12401	3.002	23.0
455	12441	3.139	23.5
460	12481	2.868	22.5

466.5	12533	3.327	24.1
470	12561	3.252	23.9
475	12600	3.145	23.5
480	12640	2.961	22.8
485	12680	3.099	23.3
490	12720	3.141	23.5
495	12760	3.266	23.9
500	12800	3.331	24.1
505	12848	4.077	26.4
510	12900	3.950	26.0
515	12953	4.460	27.4
525	13063	4.406	27.2
530	13120	3.935	26.0
535	13176	4.887	28.4
540	13233	3.955	26.0
545	13290	4.572	27.6
550	13347	4.343	27.1
560	13712	4.576	27.6
565	13786	4.470	27.4
570	13860	4.419	27.3
580	13992	3.559	24.9
585	14035	4.528	27.5
590	14077	3.925	25.9
595	14120	4.537	27.6
600	14166	4.126	26.5
605	14263	4.604	27.7
610	14361	4.234	26.8
615	14458	4.550	27.6
620	14555	4.221	26.8
630	14740	3.578	24.9
640	14894	3.432	24.5
645	14971	3.396	24.3
650	15048	3.422	24.4
655	15125	3.437	24.5
660	15202	3.779	25.5
665	15279	3.307	24.0
670	15356	3.348	24.2
675	15433	3.443	24.5
680	15510	3.386	24.3
685	15587	3.276	23.9
690	15664	3.424	24.4
695	15741	3.432	24.5
700	15818	3.494	24.7
705	15895	3.797	25.6

710	15972	3.594	25.0
715	16049	3.545	24.8
720	16126	3.434	24.5
730	16307	3.767	25.5
735	16404	3.530	24.8
740	16502	3.989	26.1
745	16600	3.721	25.3
750	16697	3.683	25.2
755.5	16805	3.449	24.5
760	16893	3.406	24.4
765	16990	3.543	24.8
770	17088	3.391	24.3
775.5	17215	3.524	24.7
780	17326	3.560	24.9
786	17473	3.576	24.9
790	17572	3.559	24.9
798	17768	3.530	24.8
800	17817	3.268	23.9
805	17940	3.411	24.4
810	18063	3.590	25.0
815.5	18198	3.447	24.5
820	18309	3.445	24.5
825	18432	3.292	24.0
830	18555	3.593	25.0
835	18678	3.406	24.4
840	18800	3.553	24.8
845	18923	3.416	24.4
850	19046	3.523	24.7
855	19169	3.411	24.4
860	19292	3.315	24.1
865	19415	3.258	23.9
870	19538	3.624	25.1
875	19661	3.268	23.9
880	19783	3.332	24.1
885	19906	3.101	23.3
890	20029	3.146	23.5
895	20152	3.223	23.8
900	20275	3.387	24.3
905	20437	3.152	23.5
910	20692	3.377	24.3
915	20946	3.106	23.3
920	21201	3.424	24.4
925	21455	3.230	23.8
930	21710	3.158	23.5

935	21964	3.370	24.3
940	22219	3.086	23.3
945	22473	3.166	23.6
950	22728	3.277	23.9
955	22982	3.112	23.4
960	23237	3.114	23.4
965	23491	3.315	24.1
970	23746	3.143	23.5
985.5	24535	3.369	24.2
990	24764	3.669	25.2

Table S3: comparison of timing of large climate transitions over the last glacial termination in the Greenland ice core GISP2 (*S16-19*), Cariaco Basin core PL07-39PC and Hulu Cave (*S20*). All ages are in calendar years BP and are based on the mid-points of the transitions. Errors in the GISP2 layer-counted chronology are estimated at 1-2% (*S21*). Errors in the GISP2 methane and Cariaco SST transition ages are calculated from the maximum age difference between the points that plausibly can be considered to mark the transition. These errors do not include errors in the absolute chronologies. Errors in GISP2 ice age – gas age differences that affect the methane ages are discussed in (*S17, S22, S23*). Errors in the Cariaco grayscale chronology are discussed in (*S9, S10*).

Transition	GISP2 ice $\delta^{18}O$	GISP2 CH_4	Cariaco 39PC SST	Cariaco 39PC Grayscale	Hulu Cave Speleothems
Late Glacial to Bølling	14,650	14,760±30† 14,630±20*	14,650±90	14,700	14,645±60
YD onset	12,860	12,770±110†	12,820±30	12,840	12,823±60
YD termination	11,630	11,610±50† 11,570±20*	11,490±70	11,560	11,473±100

†timing based on gas ages in (*S17, S18*)

*timing based on gas ages determined from the thermal diffusion signature in nitrogen and argon isotopes (*S22, S23*)

References

S1. H. L. Lin, L. C. Peterson, J. T. Overpeck, S. E. Trumbore, D. W. Murray, *Paleoceanography* **12**, 415 (1997).
S2. D. W. Lea, D. K. Pak, H. J. Spero, *Science* **289**, 1719 (2000).
S3. P. A. Martin, D. W. Lea, *Geochem Geophys Geosyst* **3**, 8401, doi:10.1029/2001GC000280 (2002).
S4. E. A. Boyle, *Geochim. Cosmochim. Acta* **47**, 1815 (1983).
S5. K. A. Hughen, J. T. Overpeck, L. C. Peterson, S. Trumbore, *Nature* **380**, 51 (1996).
S6. K. A. Hughen, J. T. Overpeck, S. J. Lehman, M. Kashgarian, J. R. Southon, *Radiocarbon* **40**, 483 (1998).
S7. M. Stuiver *et al*., *Radiocarbon* **40**, 1041 (1998).
S8. http://depts.washington.edu/qil/calib/index.html
S9. K. A. Hughen *et al*., *Nature* **391**, 65 (1998).
S10. K. A. Hughen, J. R. Southon, S. J. Lehman, J. T. Overpeck, *Science* **290**, 1951 (2000).
S11. B. E. Bemis, H. J. Spero, J. Bijma, D. W. Lea, *Paleoceanography* **13**, 150 (1998).
S12. J. F. Adkins, K. McIntyre, D. P. Schrag, *Science* **298**, 1769 (2002).
S13. L. C. Peterson, J. T. Overpeck, N. G. Kipp, J. Imbrie, *Paleoceanography* **6**, 99 (1991).
S14. M. W. Schmidt, H. J. Spero, D. W. Lea, *Geochim Cosmochim Acta* **15A Suppl. 1**, A681 (2002).
S15. T. D. Herbert, J. D. Schuffert, in *Proceedings of the Ocean Drilling Program, Scientific Results* R. M. Leckie, J. Sigurdsson, G. D. Acton, G. Draper, Eds. (2000), vol. 165, pp. 239-247.
S16. E. J. Brook, T. Sowers, J. Orchardo, *Science* **273**, 1087 (1996).
S17. E. J. Brook, S. Harder, J. Severinghaus, E. J. Steig, C. M. Sucher, *Global Biogeochem Cycles* **14**, 559 (2000).
S18. T. Blunier, E. J. Brook, *Science* **291**, 109 (2001).
S19. M. Stuiver, P. M. Grootes, *Quat. Res.* **53**, 277 (2000).
S20. Y. J. Wang *et al*., *Science* **294**, 2345 (2001).
S21. D. A. Meese *et al*., *J. Geophys. Res.* **102**, 26,411 (1997).
S22. J. P. Severinghaus, T. Sowers, E. J. Brook, R. B. Alley, M. L. Bender, *Nature* **391**, 141 (1998).
S23. J. P. Severinghaus, E. J. Brook, *Science* **286**, 930 (1999).